Enhanced interfacial Dzyaloshinskii-Moriya interaction and isolated skyrmions in the inversion-symmetry-broken Ru/Co/W/Ru films

Alexander Samardak, Alexander Kolesnikov, Maksim Stebliy, Ludmila Chebotkevich, Alexandr Sadovnikov, Sergei Nikitov, Abhishek Talapatra, Jyoti Mohanty, and Alexey Ognev

Citation: Appl. Phys. Lett. **112**, 192406 (2018); doi: 10.1063/1.5029857
View online: https://doi.org/10.1063/1.5029857
View Table of Contents: http://aip.scitation.org/toc/apl/112/19
Published by the American Institute of Physics

Enhanced interfacial Dzyaloshinskii-Moriya interaction and isolated skyrmions in the inversion-symmetry-broken Ru/Co/W/Ru films

Alexander Samardak,[1,2,a)] Alexander Kolesnikov,[1] Maksim Stebliy,[1] Ludmila Chebotkevich,[1] Alexandr Sadovnikov,[3,4] Sergei Nikitov,[3,4] Abhishek Talapatra,[5] Jyoti Mohanty,[5] and Alexey Ognev[1]

[1]*School of Natural Sciences, Far Eastern Federal University, 8 Sukhanova Str., 690950 Vladivostok, Russia*
[2]*National Research South Ural State University, 76 Lenin Prospect, 454080 Chelyabinsk, Russia*
[3]*Laboratory "Metamaterials," Saratov State University, 83 Astrakhanskaya Str., 410012 Saratov, Russia*
[4]*Kotel'nikov Institute of Radioengineering and Electronics, Russian Academy of Sciences, 11 Mokhovaya Str., 125009 Moscow, Russia*
[5]*Nanomagnetism and Microscopy Laboratory, Department of Physics, IIT Hyderabad, Kandi, 502285 Sangareddy, India*

(Received 16 March 2018; accepted 24 April 2018; published online 9 May 2018)

An enhancement of the spin-orbit effects arising on an interface between a ferromagnet (*FM*) and a heavy metal (*HM*) is possible through the strong breaking of the structural inversion symmetry in the layered films. Here, we show that an introduction of an ultrathin *W* interlayer between *Co* and *Ru* in *Ru*/*Co*/*Ru* films enables to preserve perpendicular magnetic anisotropy (PMA) and simultaneously induce a large interfacial Dzyaloshinskii-Moriya interaction (iDMI). The study of the spin-wave propagation in the Damon-Eshbach geometry by Brillouin light scattering spectroscopy reveals the drastic increase in the iDMI value with the increase in *W* thickness (t_W). The maximum iDMI of $-3.1\,\mathrm{erg/cm^2}$ is observed for $t_W = 0.24\,\mathrm{nm}$, which is 10 times larger than for the quasi-symmetrical *Ru*/*Co*/*Ru* films. We demonstrate the evidence of the spontaneous field-driven nucleation of isolated skyrmions supported by micromagnetic simulations. Magnetic force microscopy measurements reveal the existence of sub-100-nm skyrmions in the zero magnetic field. The ability to simultaneously control the strength of PMA and iDMI in quasi-symmetrical *HM*/*FM*/*HM* trilayer systems through the interface engineered inversion asymmetry at the nanoscale excites new fundamental and practical interest in ultrathin ferromagnets, which are a potential host for stable magnetic skyrmions. *Published by AIP Publishing.* https://doi.org/10.1063/1.5029857

Skyrmions are spin quasi-particles, which locally disturb the magnetic order of ferromagnets (FMs) forming a magnetization twist.[1] They can move under the action of an applied magnetic field and electrical current as real particles keeping their shape intact. This property of the topological protection allows skyrmions for prospective memory and logic applications.[2] First found in *B*20 crystals at low temperatures,[3,4] skyrmions can be nucleated in thin film structures composed of a heavy metal (HM) layer with strong spin-orbit coupling, which is in contact with an ultrathin ferromagnet.[5,6] The skyrmion stabilization at room temperature occurs through the balance between perpendicular magnetic anisotropy (PMA), interfacial Dzyaloshinskii-Moriya interaction (iDMI) and direct exchange between atoms.[7] Since the "heavy metal/ferromagnet" (*HM*/*FM*) interfaces do not induce large enough iDMI to compensate for such a deficiency, multilayer stacks with usually more than 5–10 repetitions are used.[8] The magnetostatic coupling between layers plays role of an additional energy term helping formation of skyrmions and skyrmion lattices.[9] However, this approach complicates the fabrication process and requires much more quantity of metals and hence results in increasing cost of spintronic devices. The promising solution is to use trilayer structures (HM_1/FM/HM_2) with the enhanced spin-orbit effects, including iDMI. For this reason, advanced methods of the interface modification have to be developed.

Our approach is based on the additive chiral interaction induced by the top and bottom interfaces of a HM_1/FM/HM_2 structure, where HM_1/FM and FM/HM_2 have iDMI with opposite signs.[10] But instead of the complete capping layer HM_2, we propose to use a "dusting" (ultrathin) layer of the heavy metal HM_2 covered by HM_1. This approach enables to keep robust PMA and helps to induce strong iDMI in the cost-efficient trilayer structures.[11]

In this paper, we study the influence of the *Co* and *W* thicknesses on the magnetic properties, magnetization reversal, iDMI and isolated skyrmion nucleation in the inversion-symmetry-broken *Ru*/*Co*/*W*/*Ru* films.

Our polycrystalline *Ru*/*Co*/*W*/*Ru* films were prepared by magnetron sputtering on SiO_2 substrates at room temperature. The base pressure in the chamber was 10^{-8} Torr. The working pressure of Ar^+ was 10^{-4} Torr. In order to control the thickness of layers precisely, we have used low sputtering rates: $V(Ru) = 0.011\,\mathrm{nm/s}$, $V(Co) = 0.018\,\mathrm{nm/s}$, $V(W) = 0.02\,\mathrm{nm/s}$. The *Co* thickness ($t_{Co}$) was varied from 0.7 to 1.5 nm. The thickness of the buffer and capping *Ru* layers (t_{Ru}) was 10 and 2 nm, respectively. The *W* thickness (t_W) was taken in the range from 0 to 0.4 nm. The structural and magnetic properties of the quasi-symmetrical *Ru*/*Co*/*Ru* and *Ru*/*Co*/*W*/*Ru* were systematically studied in Refs. 12 and 11, respectively.

a)E-mail: samardak.as@dvfu.ru

Brillouin light scattering (BLS) spectroscopy measurements were conducted to probe the spin-wave frequency non-reciprocity in the Damon-Eshbach geometry in order to define the iDMI's sign and value. Kerr microscopy was used to study dynamics of the domain structure of magnetic films. Kerr microscope images were captured using an immersion oil in order to increase optical resolution for clear observation of bubble-skyrmions with size as small as 700 nm.

Simultaneous atomic-force microscopy (AFM) and magnetic-force microscopy (MFM, Bruker Dimension Icon) were used to study surface morphology and magnetic domain structure of the films. The CoCr coated antimony doped Si tips (MESP) were used for MFM imaging. To prevent the tip's stray field influence of the spin textures, MFM tips with low magnetic moment (MESP-LM) were exploited.

Micromagnetic simulations of the domain structure were executed using MuMax3 software package.[13]

To extract the average iDMI values measured for large film areas, we used the Brillouin light scattering (BLS) spectroscopy of non-reciprocal propagation of spin waves in the Damon-Eshbach geometry, when a sample is in-plane magnetized and the wave vector is perpendicular to the magnetization.[14] The shift between the Stokes and anti-Stokes frequencies of spin waves of a given wavelength is directly proportional to the iDMI value[15]

$$\Delta f = f_S - f_{AS} = \frac{2\gamma}{\pi M_s} D_{eff} k_x = \frac{2\gamma D_s}{\pi M_s t_{FM}} k_x, \qquad (1)$$

where f_S and f_{AS} are the Stokes and anti-Stokes frequencies, respectively, γ is the gyromagnetic ratio, M_s is the saturation magnetization, k_x is the spin wave vector, t_{FM} is the effective ferromagnetic layer thickness considering the total thickness of magnetically dead layers of the bottom and top interfaces [$t_{FM} = t_{Co}$-($\Lambda_{Ru/Co} + \Lambda_{Co/W}$)], D_{eff} is the effective (thickness-averaged) energy density of the Dzyaloshinskii-Moriya interaction given in [erg/cm^2], $D_s = D_{eff} \cdot t_{FM}$ is the thickness-independent surface DMI constant taking into account the contributions from the bottom and top interfaces and it is given in [erg/cm].

Figure 1(a) demonstrates the typical BLS spectra for the $Ru(10)/Co(1)/W(0.25)/Ru(2)$ film (thicknesses are in nm) recorded for $k_x = 11\ \mu m^{-1}$ ($\theta \approx 28°$) in the positive and negative fields $H = \pm 5$ kOe. If a film has DMI, the spin wave frequencies will depend on the spin waves propagation direction at the fixed wave vector of the incident light as $k_x = \frac{4\pi}{\lambda} \sin\theta$, where λ is the wavelength of the light (532 nm). The effective value of DMI can be defined from Eq. (1) as

$$D_{eff} = \frac{\pi M_s \Delta f}{2\gamma k_x}, \qquad (2)$$

where $\gamma = \frac{g\mu_B}{\hbar} = g \times 87.94$ GHz/T, g is the Landé factor (for ultrathin Co films $g = 2.14$,[16] $\gamma = 188$ GHz/T). We found for $Ru(10)/Co(1)/W(0.25)/Ru(2)$ film with $M_s = 1300$ emu/cm^3 that $D_{eff} = -2.71$ erg/cm^2 and $D_s = -0.84\ 10^{-7}$ erg/cm, which are comparable to the earlier measured films: $Pt/Co/AlO_x$,[17,18] $Pt/Co/GdO_x$,[19] $Pt/CoFe/MgO$,[20] and $Pt/Co/Fe/Ir$.[9] The negative sign of iDMI supposes that the right-handed cycloidal spin

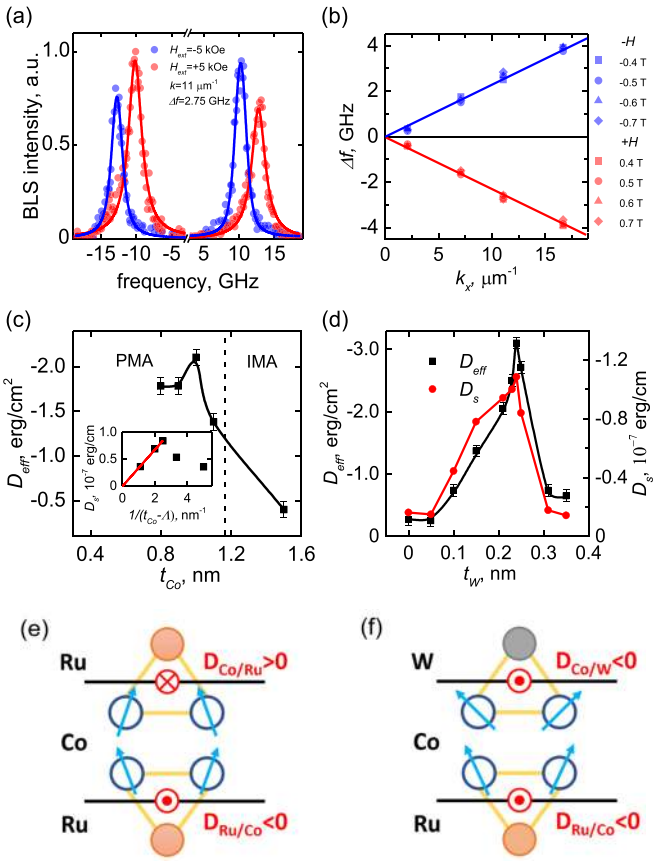

FIG. 1. (a) BLS spectra recorded for the $Ru(10)/Co(1)/W(0.25)/Ru(2)$ film. Symbols refer to the experimental data and solid lines are the Lorentzian fits. (b) Frequency shifts Δf depending on the wave vector k_x at various positive and negative applied fields for the $Ru(10)/Co(1)/W(0.25)/Ru(2)$ film. Lines are the linear approximation of the experimental data. (c) Dependence of D_{eff} on the ferromagnetic layer thickness (t_{Co}) at the fixed $t_W = 0.23$ nm. The inset demonstrate the linear decrease of $D_s = f[1/(t_{Co}\text{-}\Lambda)]$ for the relatively thick films ($t_{Co} \geq 1$ nm). (d) D_{eff} and D_s values as a function of t_W at the fixed $t_{Co} = 1$ nm. Schematic illustration of the iDMI sign dependent magnetization distribution for the bottom and top interfaces of $Ru/Co/Ru$ (e) and $Ru/Co/W$ (f) films. In the case of symmetric layers (e), the DMI vectors (marked in red) on the both interfaces are aligned antiparallel and compensate each other. For asymmetric layers (f) the DMI vectors are co-directed and the additive effect of iDMI is observed.

structures are most feasible.[21,22] The observed linear dependence of Δf on the sample tilt angle θ (or spin wave vector k_x) at various positive and negative fields H demonstrates the linear character of the spatial spin-wave dispersion imposed by the iDMI, in contrary to the quadratic dispersion that characterizes the conventional exchange interaction,[23] as shown in Fig. 1(b). The BLS spectra and $\Delta f = f(k_x, H)$ dependencies for the $Ru(10)/Co(1)/W(0.35)/Ru(2)$ film with the weak iDMI ($D_{eff} = -0.65$ erg/cm^2) are shown in Fig. S1 of the supplementary material. Slopes of $\Delta f = f(k_x)$ give the constant value of $\Delta f/k_x$, which according to Eq. (2) defines the magnitude and sign of D_{eff}. For the $Ru(10)/Co(1)/W(0.25)/Ru(2)$ film, this value is -0.24 ± 0.010 (0.24 ± 0.010) GHz/μm^{-1} for the positive (negative) field [Fig. 1(b)], which gives $D_{eff} = -2.64 \pm 0.11$ erg/cm^2. In case of the $Ru(10)/Co(1)/W(0.35)/Ru(2)$ film, the slope is -0.056 ± 0.008 (0.056 ± 0.008) GHz/μm^{-1} for the positive (negative) field giving $D_{eff} = -0.560 \pm 0.094$ erg/cm^2.

Using BLS, we studied the influence of t_{Co} and t_W on iDMI. Two series of samples were chosen: (i) with the fixed t_W and different nominal thickness of the ferromagnetic

layer—$Ru(10)/Co(t_{Co})/W(0.23)/Ru(2)$; (ii) with the fixed t_{Co} and various t_W—$Ru(10)/Co(1)/W(t_W)/Ru(2)$. Figure 1(c) shows the dependency of D_{eff} on the t_{Co}. For the thickness range of t_{Co} below 1.0 nm, where PMA exists, DMI has nonlinear dependence caused by the structural inhomogeneity of ultrathin *Co* layers, whose effective thickness is below the lattice constant of *Co–hcp* (c = 0.406 Å). At $t_{Co} > 1.17$ nm, the in-plane magnetic anisotropy appears and the iDMI value significantly decreases down to -0.4 erg/cm^2 for $t_{Co} = 1.5$ nm. The interfacial origin of iDMI is proven by the linear decrease of $D_s = f[1/(t_{Co}\text{-}\Lambda)]$ for $t_{Co} > 1$ nm [see the inset in Fig. 1(c)]. The peak iDMI value ($D_{eff} = -2.1$ erg/cm^2) was observed for $t_{Co} = 1$ nm, at which the *Co* layer becomes structurally homogeneous. For this particular *Co* thickness, we studied the dependencies of D_{eff} and D_s as a function of t_W [Fig. 1(d)]. For the quasi-symmetrical $Ru(10)/Co(1)/Ru(2)$, the value of D_{eff} is -0.27 erg/cm^2. The existence of the non-zero negative iDMI points out the different morphological quality (roughness, intermixing depth) of the *Ru/Co* and *Co/Ru* interfaces, as it was revealed for *Pt/Co/Pt* trilayers.[24,25] We found for *Ru/Co/Ru* films that if the thickness of the *Ru* capping decreases down to 0.5 nm, the value of D_{eff} increases up to -1.31 erg/cm^2. Due to the very thin *Ru* capping, surface oxygen atoms can penetrate into the *Co* layer and partially oxidize its top interface. This assumption is supported by the fact that this sample still has strong PMA, but the coercive field and saturation magnetization are about 22 and 14% less than for the same structure with the 2-nm thick *Ru* capping (see Fig. S2 in the supplementary material). Since the slight magnetic layer oxidation does not contribute or even decreases the net iDMI, as it has been recently shown in Ref. 26, we can assume that in our particular case the iDMI contribution from the top *Co/Ru* interface with $M_s = 950$ emu/cm^3 is negligible ($D_{Co/Ru} \approx 0$) and $D_{eff} = -1.31$ erg/cm^2 is mostly induced by the bottom *Ru/Co* interface. It means, that in case of the quasi-symmetric *Ru/Co/Ru* films with the 2-nm thick *Ru* capping and $M_s = 1100$ emu/cm^3, the top *Co/Ru* interface has the positive DMI with the value defined as $D_{Co/Ru} = D_{eff[Ru(10)/Co(1)/Ru(2)]} - D_{Ru/Co} = -0.27 + 1.31 = 1.04$ erg/cm^2. A scheme illustrating the cancelation of iDMI in the symmetrical *Ru/Co/Ru* film is represented in Fig. 1(e).

The introduction of the *W* interlayer with thickness up to 0.24 nm allows considerable enhancement of structural inversion asymmetry in *Ru/Co/W/Ru* films resulting in more than 10 times increase of D_{eff}. The peak value -3.1 erg/cm^2 was observed for $t_W = 0.24$ nm. In the range $0.24\text{ nm} < t_W < 0.31$ nm we found the abrupt fall of D_{eff} down to -0.74 erg/cm^2 accompanied by the decrease of K_{eff} as shown in Ref. 11.

We propose that the sharp increase of D_{eff} is provoked by the additive effect of *Ru/Co* and *Co/W* interfaces, due to *Ru/Co* and *W/Co* interfaces have opposite signs of DMI: negative for *Ru* and positive for *W*. This means that $D_{Ru/Co} < 0$ and $D_{Co/W} < 0$, as illustrated in Fig. 1(f). We have determined the iDMI value of the *Co/W* interface for $Ru(10)/Co(1)/W(0.24)/Ru(2)$ as $D_{Co/W} = D_{eff}\text{-}D_{Ru/Co} = -3.1 + 1.31 = -1.79$ erg/cm^2. The decrease of D_{eff} for $t_W > 0.24$ nm is due to the increase of the magnetically dead layer on the *Co/W* interface,[11] which leads to consequent degradation of the *Co* layer.

In order to compare the iDMI values for different systems, the interfacial constant D_s has to be calculated for the effective thickness of the ferromagnetic layer taking into account the accurately defined magnetically dead layers of the bottom and top interfaces, Fig. 1(d). Otherwise, the D_s value can be significantly overestimated, when the nominal thickness is in use. It is important that *Ru/Co/W/Ru* films with $0.8\text{ nm} < t_{Co} < 1.17$ nm and $0.15\text{ nm} < t_W < 0.3$ nm can be used for the isolated skyrmion stabilization.[7,10] This can happen in these films due to the iDMI values, which are near the critical energy density for the formation of the chiral domain walls written as $D_{cr} = \frac{4}{\pi}\sqrt{AK_{eff}}$,[27,28] where *A* is the exchange stiffness constant.

Since the constant *A* was not measured for our ultrathin films, we used the wide range of known values of *A* for pure *Co* from 1 to 3×10^{-6} erg/cm.[29] For a sample with $K_{eff} = 0.6 \times 10^6$ erg/cm^3, one can find that D_{cr} varies from 0.98 to 1.71 erg/cm^2. Accordingly,[7,10] our modified *Ru/Co/W/Ru* films with t_W ranging from 0.15 to 0.25 nm can be potentially used for the nucleation and manipulation of homochiral Néel domain walls and isolated skyrmions, making the realization of the skyrmionic memory and domain wall based devices.

For the creation and stabilization of skyrmions in thin films, a unique combination of the magnetic parameters, such as PMA, Heisenberg exchange, M_s, and iDMI, is required.[22,30–32] Due to the lack of the iDMI strength, a multilayer configuration of films with the magnetostatically coupled layers is usually used for the skyrmion stabilization and manipulation.[7] This coupling leads to a sheared hysteresis loop with $M_r/M_s \approx 0$, as demonstrated for one of our multilayer (the same behavior was found in Ref. 33) in Fig. S3 of the supplementary material. This is due to the formation of equilibrium multidomain state. But this is not a case of the $HM_1/FM/HM_2$ trilayers as shown in Fig. S3(c) of the supplementary material.

We found by means of polar Kerr effect microscopy that iDMI stabilized isolated skyrmions in the *Ru/Co/W/Ru* films with $t_{Co} = 1.1$ nm, which have relatively weak PMA ($K_{eff} \approx 0.3 \times 10^6$ erg/cm^3). Figure 2 shows the out-of-plane field driven evolution of the magnetic domain structure in the $Ru(10)/Co(1.1)/W(0.25)/Ru(2)$ film. The large area images of the domain structure are shown in Fig. S4 of the supplementary material.

To nucleate skyrmions, we used the following technique. First, the sample was demagnetized in the out-of-plane field (H_z) with an amplitude decreasing to zero. Then, the field was smoothly increased to a field larger than $-H_c$, but a bit smaller than $-H_s$. In this case, the domain structure "collapses," but bubble-skyrmions remain. When the magnetic field H_z was reduced to zero, we observed isolated skyrmions with the smallest size of about 700 nm [see Fig. 2(a)] owing to the limited optical resolution of our Kerr microscope. With the increasing field up to $H_z = -20$ Oe, most of the skyrmions keep their position and shape that proves their stability [Figs. 2(b) and 2(c)]. In the field $H_z > -30$ Oe, the size of domains sharply increased [Figs. 2(e) and 2(f)]. The supplementary material to the article contains two movies

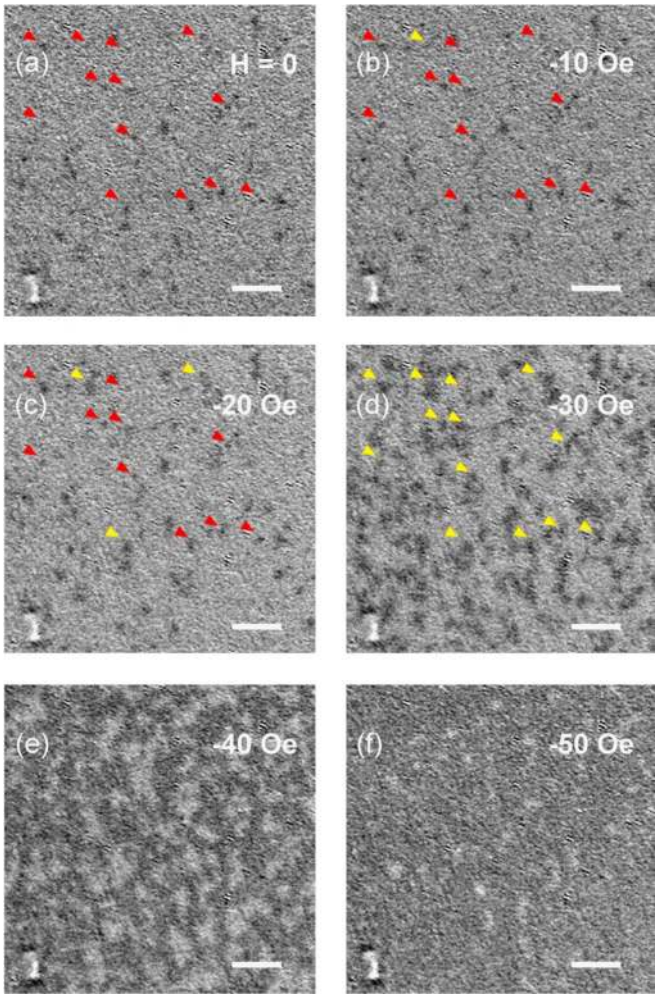

FIG. 2. Magnetic domain structure of the *Ru*(10)/*Co*(1.1)/*W*(0.25)/*Ru*(2) film captured in the out-of-plane field by Kerr microscopy. The red arrows indicate skyrmions, which grow and form domains marked by the yellow arrows. The scale bar is 5 μm.

demonstrating the magnetization reversal process from $+H_s$ to $-H_s$ (Movie 1) and the formation of skyrmions and their stabilization at zero field (Movie 2).

To prove the skyrmion formation in the *Ru*/*Co*/*W*/*Ru* trilayers, we have performed micromagnetic simulations of the 4×4 μm^2 area of films using the continuous boundary conditions. Recently, we have demonstrated that at the *Ru* buffer layer thickness of 10 nm, the *Co* films are polycrystalline[12] in nature. It leads to the local variation of magnetic properties and finally, can result in increased critical fields, namely, the coercive force due to the domain wall pinning. Therefore, magnetic inhomogeneities in disordered films can pin skyrmions or change their shape and size.[34–36] In the simulations we considered the variation of the crystallographic anisotropy $K_1 = 1.0 \times 10^6$ erg/cm^3 on the grains with size of 20 nm.[12,35] The orientation of the easy axis of magnetization was assigned randomly for each crystallite and the value of K_1 was varied within $\pm 10\%$. A distribution map of the crystallographic anisotropy constant K_1 used for micromagnetic simulations is shown in Fig. S5 of the supplementary material. We used the following parameters: $/D_{eff}/ = 1.0$ erg/cm^2, which is within the range of possible magnitudes of $D_{cr} = 0.7$–1.2 erg/cm^2 for this film, $M_s = 1300$ emu/cm^3, $K_{eff} = 0.3 \times 10^6$ erg/cm^3, $A = 1.6 \times 10^{-6}$ erg/cm, and the cell size $4 \times 4 \times 0.5$ nm^3. According to Ref. 7, films with $D_{eff}/D_{cr} < 1$ can be a host of isolated skyrmions, which we observed in our trilayers in the absence of a magnetic field [Fig. 2(a)]. The random size and spatial distribution of skyrmions reflects the fact that the iDMI value can be lower than D_{cr}. To realize a stable skyrmion lattice, the ratio of D_{eff}/D_{cr} has to be larger than 2.[7]

At the beginning, the six isolated skyrmions were created in zero field [Fig. 3(a)]. One can see that the shape and size of skyrmions are different because of the magnetic inhomogeneities. The average skyrmion diameter is 224 nm. All the skyrmions have the skyrmion number $N_{sk} = 1$. With the rising magnetic field up to 30 Oe, the shape of 4th and 5th skyrmions significantly changed; meantime, the size of 2nd and 3rd skyrmions increased. In the fields of 40 and 50 Oe only 3rd skyrmion became unchanged. Further increase of the field [Figs. 3(e) and 3(f)] promoted the sharp growth of skyrmions and their transformation into large domains. The very similar behavior was observed experimentally (Fig. 2). We found that without consideration of disorders in films, skyrmions were unstable in zero magnetic field and they immediately transformed into domains.

We have done MFM experiments without any applied magnetic field ($H_z = 0$), which prove the spontaneous isolated skyrmion formation as demonstrated in Fig. 4(b)

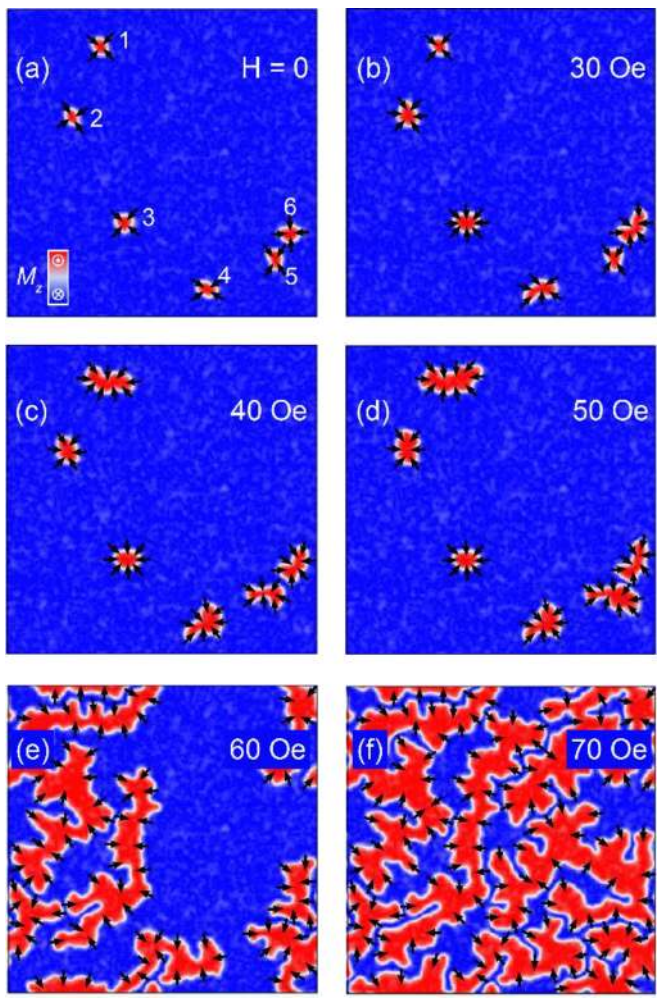

FIG. 3. Simulated images of the out-of-plane field driven domain structure of the *Ru*(10)/*Co*(1.1)/*W*(0.25)/*Ru*(2) film. The image size is 4×4 μm^2.

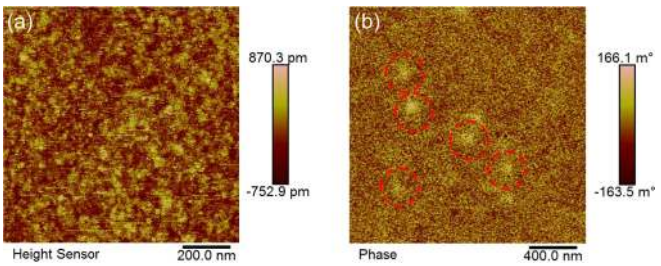

FIG. 4. AFM (a) and MFM (b) images captured on the *Ru*(10)/*Co*(0.9)/*W*(0.25)/*Ru*(2) film at the remnant state ($H_z = 0$).

(marked by circles). The size of skyrmions are about 100 nm, which is consistent with the previous findings.[7] The difference in size of skyrmions observed by MFM and Kerr microscopy is due to the different nucleation procedure used and the higher spatial resolution of a magnetic tip.

Our study of the broken structural inversion symmetry *Ru*/*Co*/*W*/*Ru* films has unveiled the thicknesses of *Co* and *W* layers for which the robust PMA exists and the iDMI remarkably enhances (up to $-3.1\,\mathrm{erg/cm^2}$) thanks to the additive chiral interaction on interfaces. The introduction of the *W* interlayer into the top *Co*/*Ru* interface decreases the elastic strains in the ferromagnetic layer, smoothens the *Co* surface, and dramatically decreases the coercive force. The created unique combination of structural and magnetic parameters enables to nucleate and stabilize isolated skyrmions in the films with only one ultrathin ferromagnetic layer in the zero field. For the realization of a stable skyrmion lattice, we suggest a magnetostatically coupled multilayer film based on repetition of the *Ru*/*Co*/*W*/*Ru* structure. Our findings show the high potential of *Ru* as a worthy alternative to *Pt* and open up the way for the extensive interface engineering at the nanoscale in order to tune the magnetic properties and to strengthen the spin-orbit effects for the future spin-orbitronic applications, especially for skyrmionic devices.

See supplementary material for the additional figures from Fig. S1 to Fig. S5 and for Movie 1 showing the remagnetization process in the out-of-plane field and Movie 2 demonstrating the field-driven skyrmion formation.

This work has been partially supported by the Russian Foundation for Basic Research (Grant No. 17-52-45135), the Russian Ministry of Education and Science under the state tasks (Nos. 3.5178.2017/8.9 and 3.4956.2017), the Grant program of the Russian President (No. MK-2643.2017.2), Act 211 of the Government of the Russian Federation (Contract No. 02.A03.21.0011), and the INT/RUS/RFBR/P-273 grant.

[1]N. Nagaosa and Y. Tokura, Nat. Nanotechnol. **8**, 899 (2013).
[2]J. P. Liu, Z. Zhang, and G. Zhao, *Skyrmions: Topological Structures, Properties, and Applications*, Series in Materials Science and Engineering (CRC Press, Taylor & Francis Group, 2016), p. 482.
[3]S. Mühlbauer, B. Binz, F. Jonietz, C. Pfleiderer, A. Rosch, A. Neubauer, R. Georgii, and P. Böni, Science **323**, 915 (2009).
[4]X. Z. Yu, Y. Onose, N. Kanazawa, J. H. Park, J. H. Han, Y. Matsui, N. Nagaosa, and Y. Tokura, Nature **465**, 901 (2010).
[5]W. Legrand, D. Maccariello, N. Reyren, K. Garcia, C. Moutafis, C. Moreau-Luchaire, S. Collin, K. Bouzehouane, V. Cros, and A. Fert, Nat. Nanotechnol. **13**, 233 (2018).
[6]W. Jiang, G. Chen, K. Liu, J. Zang, S. G. E. te Velthuis, and A. Hoffmann, Phys. Rep. **704**, 1 (2017).
[7]A. Fert, N. Reyren, and V. Cros, Nat. Rev. Mater. **2**, 17031 (2017).
[8]A. Manchon and A. Belabbes, in *Solid State Physics*, edited by R. E. Camley and R. L. Stamps (Academic Press, 2017), p. 1.
[9]A. Soumyanarayanan, M. Raju, A. L. Gonzalez Oyarce, A. K. C. Tan, M.-Y. Im, A. P. Petrović, P. Ho, K. H. Khoo, M. Tran, C. K. Gan *et al.*, Nat. Mater. **16**, 898 (2017).
[10]C. Moreau-Luchaire, C. Moutafis, N. Reyren, J. Sampaio, C. A. F. Vaz, N. Van Horne, K. Bouzehouane, K. Garcia, C. Deranlot, P. Warnicke *et al.*, Nat. Nanotechnol. **11**, 731 (2016).
[11]A. G. Kolesnikov, A. V. Ognev, M. E. Stebliy, L. A. Chebotkevich, A. V. Gerasimenko, and A. S. Samardak, J. Magn. Magn. Mater. **454**, 78 (2018).
[12]A. G. Kolesnikov, M. E. Stebliy, A. V. Ognev, A. S. Samardak, A. N. Fedorets, V. S. Plotnikov, X. F. Han, and L. A. Chebotkevich, J. Phys. D: Appl. Phys. **49**, 425302 (2016).
[13]A. Vansteenkiste, J. Leliaert, M. Dvornik, M. Helsen, F. Garcia-Sanchez, and B. V. Waeyenberge, AIP Adv. **4**, 107133 (2014).
[14]J.-H. Moon, S.-M. Seo, K.-J. Lee, K.-W. Kim, J. Ryu, H.-W. Lee, R. D. McMichael, and M. D. Stiles, Phys. Rev. B **88**, 184404 (2013).
[15]J. Cho, N.-H. Kim, S. Lee, J.-S. Kim, R. Lavrijsen, A. Solignac, Y. Yin, D.-S. Han, N. J. J. van Hoof, H. J. M. Swagten *et al.*, Nat. Commun. **6**, 7635 (2015).
[16]M. A. W. Schoen, J. Lucassen, H. T. Nembach, T. J. Silva, B. Koopmans, C. H. Back, and J. M. Shaw, Phys. Rev. B **95**, 134410 (2017).
[17]M. Belmeguenai, J.-P. Adam, Y. Roussigné, S. Eimer, T. Devolder, J.-V. Kim, S. M. Cherif, A. Stashkevich, and A. Thiaville, Phys. Rev. B **91**, 180405 (2015).
[18]N. H. Kim, J. Jung, J. Cho, D. S. Han, Y. X. Yin, J. S. Kim, H. J. M. Swagten, and C. Y. You, Appl. Phys. Lett. **108**, 142406 (2016).
[19]M. Vaňatka, J. C. Rojas-Sánchez, J. Vogel, M. Bonfim, M. Belmeguenai, Y. Roussigné, A. Stashkevich, A. Thiaville, and S. Pizzini, J. Phys.: Condens. Matter **27**, 326002 (2015).
[20]M. Belmeguenai, M. S. Gabor, Y. Roussigné, A. Stashkevich, S. M. Chérif, F. Zighem, and C. Tiusan, Phys. Rev. B **93**, 174407 (2016).
[21]S. Emori, U. Bauer, S.-M. Ahn, E. Martinez, and G. S. D. Beach, Nat. Mater. **12**, 611 (2013).
[22]H. Yang, A. Thiaville, S. Rohart, A. Fert, and M. Chshiev, Phys. Rev. Lett. **115**, 267210 (2015).
[23]A. A. Stashkevich, M. Belmeguenai, Y. Roussigné, S. M. Cherif, M. Kostylev, M. Gabor, D. Lacour, C. Tiusan, and M. Hehn, Phys. Rev. B **91**, 214409 (2015).
[24]A. W. J. Wells, P. M. Shepley, C. H. Marrows, and T. A. Moore, Phys. Rev. B **95**, 054428 (2017).
[25]M. Quinsat, Y. Ootera, T. Shimada, M. Kado, S. Hashimoto, H. Morise, S. Nakamura, and T. Kondo, AIP Adv. **7**, 056318 (2017).
[26]D. de Souza Chaves, F. Ajejas, V. Krizakova, J. Vogel, and S. Pizzini, e-print arXiv:1708.08516v1.
[27]M. Heide, G. Bihlmayer, and S. Blügel, Phys. Rev. B **78**, 140403 (2008).
[28]S. Rohart and A. Thiaville, Phys. Rev. B **88**, 184422 (2013).
[29]C. Eyrich, W. Huttema, M. Arora, E. Montoya, F. Rashidi, C. Burrowes, B. Kardasz, E. Girt, B. Heinrich, O. N. Mryasov *et al.*, J. Appl. Phys. **111**, 07C919 (2012).
[30]B. Dupe, G. Bihlmayer, M. Bottcher, S. Blugel, and S. Heinze, Nat. Commun. **7**, 11779 (2016).
[31]G. Yu, P. Upadhyaya, X. Li, W. Li, S. K. Kim, Y. Fan, K. L. Wong, Y. Tserkovnyak, P. K. Amiri, and K. L. Wang, Nano Lett. **16**, 1981 (2016).
[32]A. G. Kolesnikov, A. S. Samardak, M. E. Stebliy, A. V. Ognev, L. A. Chebotkevich, A. V. Sadovnikov, S. A. Nikitov, Y. J. Kim, I. H. Cha, and Y. K. Kim, J. Magn. Magn. Mater. **429**, 221 (2017).
[33]S. Woo, K. M. Song, H.-S. Han, M.-S. Jung, M.-Y. Im, K.-S. Lee, K. S. Song, P. Fischer, J.-I. Hong, J. W. Choi *et al.*, Nat. Commun. **8**, 15573 (2017).
[34]M. Baćani, M. A. Marioi, J. Schwenk, and H. J. Hug, e-print arXiv:1609.01615.
[35]W. Legrand, D. Maccariello, N. Reyren, K. Garcia, C. Moutafis, C. Moreau-Luchaire, S. Collin, K. Bouzehouane, V. Cros, and A. Fert, Nano Lett. **17**, 2703 (2017).
[36]J.-V. Kim and M.-W. Yoo, Appl. Phys. Lett. **110**, 132404 (2017).